Journal of Clinical Orthopaedics and Trauma 20 (2021) 101493

Contents lists available at ScienceDirect

Journal of Clinical Orthopaedics and Trauma

journal homepage: www.elsevier.com/locate/jcot

Methods to address metal artifacts in post-processed CT images – A *do-it-yourself* guide for orthopedic surgeons

Siddhartha Sharma [1], Aditya Kaushal [1], Sandeep Patel[*], Vishal Kumar, Mahesh Prakash, Dhillon Mandeep

Department of Orthopedics, Postgraduate Institute of Medical Education and Research, Chandigarh, India

ARTICLE INFO

Article history:
Received 1 June 2021
Received in revised form
29 June 2021
Accepted 30 June 2021
Available online 1 July 2021

Keywords:
CT scan
Metal artifact
Metal artifact reduction
Windowing
Segmentation
Multiplanar reformat
3D modeling

ABSTRACT

Computed tomography (CT) scans are often used for postoperative imaging in orthopedics. In the presence of metallic hardware, artifacts are generated, which can hamper visualization of the CT images, and also render the study ineffective for 3-D printing. Various solutions are available to minimize metal artifacts, and radiologists can employ these before or after processing the CT study. However, the orthopedic surgeon may be faced with situations where the metal artifacts were not addressed. To counter such problems, we present three *do-it-yourself* (DIY) techniques that can be used to manage metal artifacts.

1. Introduction

Cross-sectional imaging by Computed Tomographic (CT) Scan plays a crucial role in diagnosing, planning, managing, and follow-up of orthopedic patients.[1–3] Postoperative CT imaging may be indicated for several reasons. In periarticular fractures, postoperative CT is used to judge the accuracy of reduction and evaluate possible joint penetration of screws.[4,5] In spinal surgery, it may be used to assess pedicle screw penetration into the spinal canal or possible vertebral artery injury in cases of cervical spine instrumentation.[6] In arthroplasty practice, it is commonly used to assess aseptic as well as septic loosening.[7,8] Postoperative CT is also increasingly used to evaluate fracture union[9,10] and progression of arthrodesis.[11] However, metallic artifacts due to orthopedic implants hinder the visualization and, subsequently, the diagnostic yield of CT images.[12,13] These artifacts are generally seen as bright and dark streaks in CT sections and cause a significant impairment of image quality and obscuration of local anatomic structures.[14] Moreover, such artifacts also render advanced planning techniques such as virtual 3D reconstruction and rapid prototyping unusable. Although several methods have been developed to minimize metal-induced artifacts in postoperative CT scans, most of these work at the time of image acquisition or immediately after acquisition (post-processing).

Occasionally, the orthopedic surgeon may be faced with the situation where postoperative CT imaging has been performed without attempting to address the metal artifacts. Repeating the scan in such a situation would not only subject the patient to radiation, it would also add to the cost of treatment. In this article, we will briefly describe methods that orthopedic surgeons can use to get the desired information in such situations.

2. Genesis of metal artifacts

The major causes of metal artifacts include *photon starvation* and *beam hardening*. These phenomena occur primarily due to the fact that metallic hardware has a higher density as compared to the surrounding tissues. Moreover, more pronounced metallic artifacts can also be noticed in alloys having higher atomic number such as stainless steel or cobalt, in contrast to alloys containing Titanium, which has a lower atomic number.[15]

* Corresponding author. Department of Orthopedics, PGIMER, Chandigarh, Pin-160012, India.
E-mail address: sandeepdrpatelortho@gmail.com (S. Patel).
[1] Joint first authors.

https://doi.org/10.1016/j.jcot.2021.101493
0976-5662/

Photon starvation occurs due to beam attenuation, which depends on the frequency of photoelectric effect and Compton scatter, which are the primary means of interaction between the X-Ray beam and matter at the beam energy levels used in diagnostic imaging. In the *photoelectric effect*, an incident photon transfers all its energy to and ejects a K-shell electron, thus getting absorbed in the process.[15] As the photoelectric effect is proportional to the cube of the atomic number, it is markedly amplified in metals in comparison to the surrounding soft tissues. Hence, this results in to fewer X-Ray photons reaching the imaging detectors from the area of the metallic hardware. The *Compton effect* occurs as a result of deviation of photons from the original trajectory, producing signals in different detectors rather than the one in line with the trajectory leading to scatter artifacts. These phenomena can be seen in the scan as alternate bright and dark streaks in the reconstructed images,[16] thus reducing contrast and signal-to-noise ratio (SNR).[17]

Another important cause of metal artifacts is *beam hardening*, which occurs due to polychromaticity (combination of low as well as high-energy photons) of the X-Ray beam.[15,18] Low-energy photons are easily attenuated, particularly when travelling through matter with a high atomic number like metal. The resultant beam is therefore composed of only higher-energy photons.

Overall, the combination of photon starvation and beam hardening in areas around metallic implants leads to inconsistent data acquisition, with resultant dark streaks near metallic implants.[15]

3. Usual strategies to address metal artifacts in CT scans

Correction of metallic artifacts can be done either in the pre or post-acquisition phases. *Pre-acquisition reduction* of artifacts may be achieved by either increasing the tube current (mAs setting), which will allow a greater number of incident photons to pass through the metal, or by increasing the peak voltage (kVp setting) which will increase the mean energy of the incident beam. However, these methods reduce the artifacts by only a minor degree.[14,19] And also increase the radiation dose received by the patient.[15] Modern CT systems also have different inbuilt features to address beam hardening. These include filtration, calibration, correction and correction software.[15] A recent innovation is the Dual Energy CT (DECT) scanner. Whereas conventional CT scanners use a single X-Ray photon energy spectrum; DECT uses two different X-Ray photon energy spectra. Therefore, it allows for assessment of attenuation coefficients at varying energy spectra, and has the ability to reduce beam polychromaticity and beam hardening, with no significant increase in the patient radiation dose.[20–22]

Post-acquisition artifact reduction methods, as the name suggests, are deployed after acquisition of raw images, and work on software based algorithms to weed out artifacts. These algorithms work by detection and segmentation (isolation) of the image data responsible for artifacts, and its subsequently modification with the estimated correct value. Image-based segmentation methods are used most commonly; here, the metal pixels are segmented by determining attenuation thresholds. Most of the modern CT machines are equipped with such software-based Metal Artifact Reduction (MAR) algorithms (for e.g., O-MAR, iMAR), which are provided by the vendors themselves.[23,24]

4. Do-it-yourself strategies to address metal artifacts in post-processed CT scans

Whereas metal artifacts may be addressed in the pre-acquisition phase, or by using the vendor based software provided within the CT machine after acquisition, the orthopaedic surgeon may be faced with the situation where artifacts have not been addressed. What can the orthopedic surgeon do in such situations? We present three techniques that can be used to save the day (Table 1). Whereas the first two techniques require minimal technical knowledge and can be accomplished quickly, the third requires a good understanding and experience with image processing, and is more time consuming. It must be remembered that orthopedic surgeons must have access to the CT data in the DICOM format to be able to use any of these techniques.

a. Windowing

This method involves alterations in brightness and contrast of the displayed image. It is quick, easy and intuitive, and can often render artifact studded images suitable for viewing on-screen. However, this does not alter the actual CT image data, and is therefore not suited for advanced applications like 3-D printing. A few key concepts are presented for better understanding of this technique.

The *pixel* is the smallest unit of a two-dimensional digital image. Each CT image is composed of millions of pixels, and each pixel has its own brightness, or radiodensity. The three-dimensional equivalent of a pixel is a *voxel*.[25] Radiodensity in CT Scans is quantified by means of the Hounsfield Unit (HU), which depends on the absorption/attenuation coefficient of the tissue under consideration. Distilled water (at a standardized temperature and pressure) is arbitrarily assigned a HU value of 0, whereas air is designated as −1000. Denser the tissue, higher its HU value, and vice versa. Hence, bone has higher HU value than soft tissues, and metal has the highest HU values.[26]

Windowing is a process by which the HU values of an image is manipulated to alter its appearance, in order to a highlight anatomical structures of interest. Windowing is achieved by altering the *window level* (WL) and *window width* (WW). The window level is used to alter the image brightness, whereas the window width is used to alter the contrast. The window width is the difference between the lowest and highest HU pixels of the image. Therefore, if the window width is higher, a wider range of pixels will be displayed, and vice-versa.[27] In the presence of metal hardware, choosing a wider window that encompasses the high HU values of metal, as well as the lower HU values of the bone will generally allow good visualization of the metal-bone interface. A step-by-step guidance on this technique is presented below (Fig. 1). In this example, the HOROS DICOM Viewer (https://horosproject.org/) has been used.

- An axial section from a postoperative CT scan of a patient who underwent pedicle screw fixation is depicted. The default window level is set to 'CT Bone', which is commonly used for orthopedic CTs. The surgeon wants to know if there is any breach of the spinal canal by the pedicle screw. At the current display settings, metal artifacts are visible, and obscure visualization of the screw-canal relationship (Fig. 1a).
- The HU value of the metal is identified. This can be done drawing an oval or rectangle in the region of interest. The minimum, maximum and mean HU values are displayed. (in this example, minimum HU = 2393, maximum HU = 3071 and mean HU = 2926.35) (Fig. 1a)
- The HU value of the bone is identified in a similar fashion. (in this example, minimum HU = 308, maximum HU = 518 and mean HU = 375.05) (Fig. 1b)
- The window width is altered to incorporate the overall minimum HU value (which is 308 in this case) and the overall maximum HU value (which is 3071 in this case) from the two region of interests marked previously. The window width is therefore set from 308 to 3071, and is 2763 (i.e. 3071 − 308) (Fig. 1c).

Table 1
Overview of do-it-yourself metal artifact reduction techniques presented in the paper.

SNo.	Technique	Software Needed	Approximate Time Needed	Uses	Difficulty Level
1.	Windowing	DICOM Viewer (for e.g., HOROS)	<5 min	Visualization	Beginner
2.	Minimum Intensity Projection with thick slab (Multiplanar reformatting)	DICOM viewer (for e.g., HOROS)	<5 min	Visualization	Beginner
3.	Segmentation	Image Processing Software (for e.g., MIMICS or 3D Slicer)	30–60 min, depending on the complexity	Virtual 3D models, 3D printing	Advanced

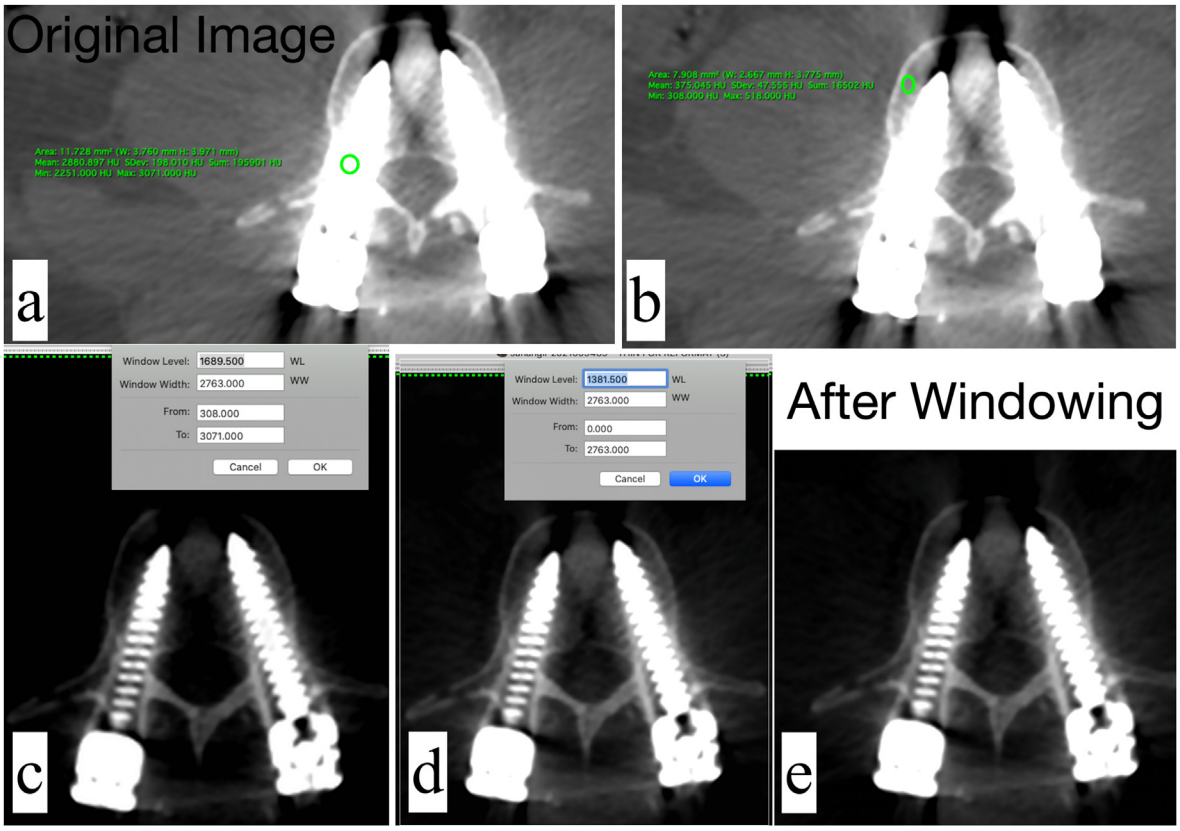

Fig. 1. Application of the windowing technique to address metal artifacts in a patient with postoperative spine CT. a) The unprocessed axial section – artifacts are noted around the pedicle screw. The oval region of interest (ROI) tool has been placed over the pedicle screw, it's HU values are displayed in the green text. b) The oval ROI tool has been positioned over the vertebral body, the corresponding HU values are displayed. c) The window width has been adjusted. d) The window level has been adjusted e) The final image, showing reduction of metal artifacts.

- The window level is set to 50% of the window width (i.e. 2763/2 = 1381.5) (Fig. 1d). This brightens up the image sufficiently, while minimizing the artifacts from the pedicle screw. The relationship of the screw with the canal can be now appreciated well, and it is noted that there is no canal breach by either screw (Fig. 1e).

b. Artifact reduction on Multiplanar Reformats – Minimum Intensity Projection with *thick slab*

Multiplanar reformation is the process of obtaining non-axial sections from axial sections. Typically, coronal and sagittal reformatted images are used in orthopedic practice, although it is also possible to generate oblique and curved plane images.[28] Reformatted images are generated from a single axial section which is only one voxel in thickness. This is achieved by extrapolating a ray passing from the section at a pre-defined angle to the viewer's eye. A '*thick slab*' is generated by taking several axial sections into account, and most DICOM viewer software allow users to adjust the slab thickness. The way in which MPR images are displayed can be altered by choosing one of the several commonly available algorithms, one such algorithm is the Minimum Intensity Projection (MinIP). In this algorithm, the most hypodense structures are displayed.[28] Since metal has high HU value, the MinIP projection results in suppression of high intensity voxels, and improves visualization of the surrounding bone. By increasing the slab thickness, artifacts can be minimised further. As is the case with windowing, this technique does not alter the CT data, it only alters the image displayed on the screen. A step-by-step guidance on this technique is presented below (Fig. 2). The case illustrated previously (Section 3a) is used. In this example, the HOROS DICOM Viewer (https://horosproject.org/) has been used.

- The 2D orthogonal MPR function is chosen to generate MPRs from the axial slices. By default, the software generates MPR with the Maximum Intensity Projection (MIP). The metal artifacts are clearly visible in this mode.

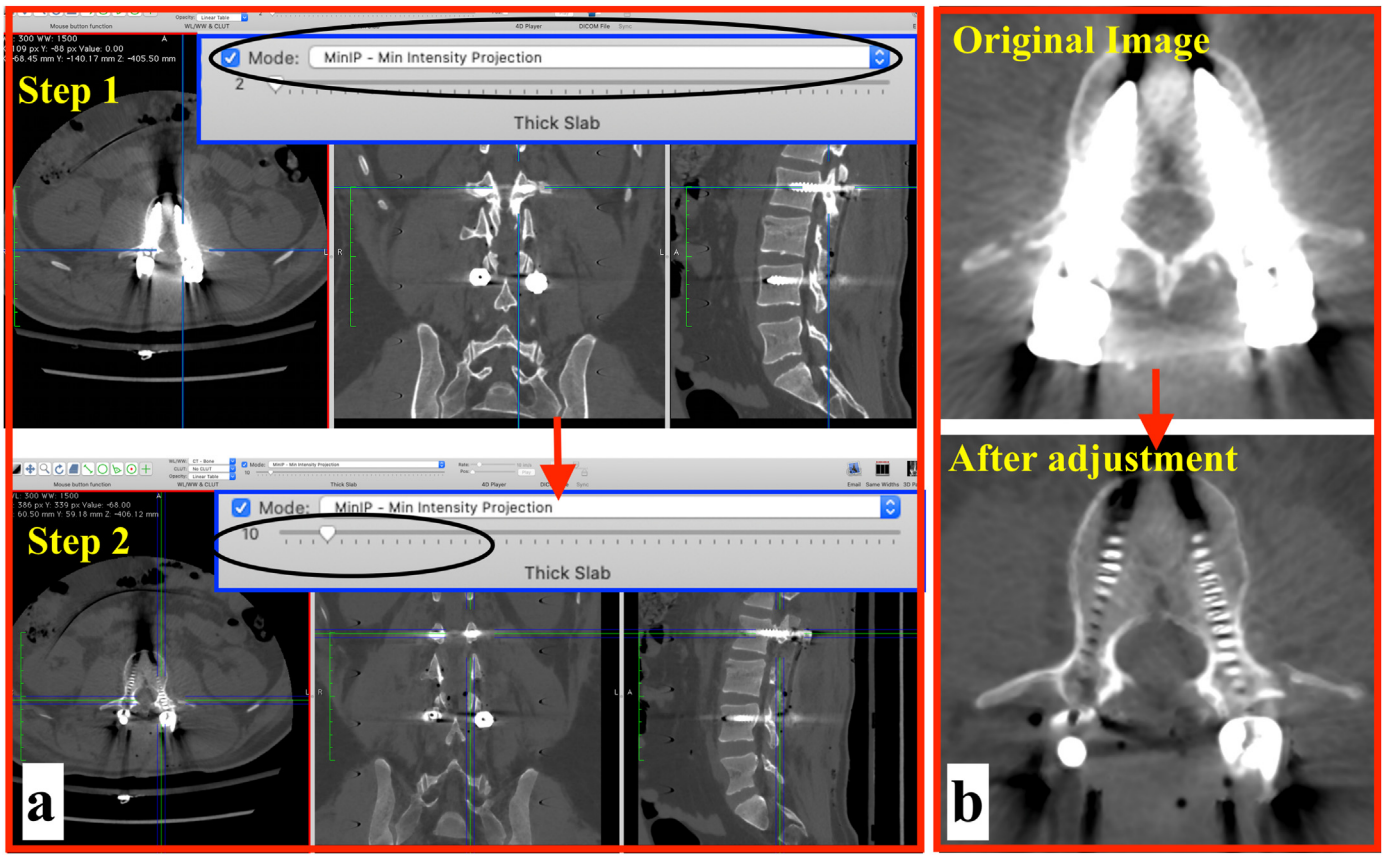

Fig. 2. Application of the Minimum Intensity Projection with Thick Slab technique. a) Minimum intensity projection mode is selected (Step 1). This is followed by increasing the slab thickness from 2 to 10 (Step 2). b) Before and after comparison, showing reduction of metal artifacts.

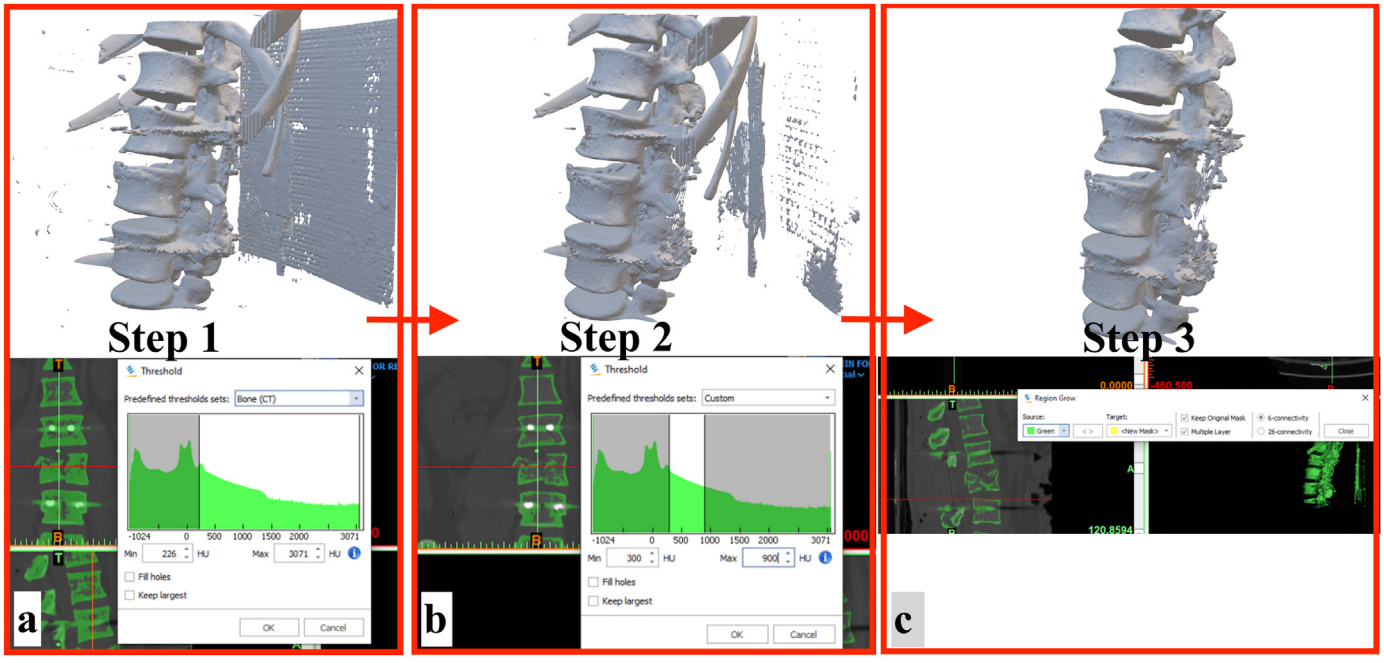

Fig. 3. 3D editing in the MIMICS software. a) The study is imported into the software, default threshold settings (Bone CT) are in place b) The default threshold settings are changed to exclude metal from the study c) The 'Region Grow' tool is used to generate to perform segmentation. The effect of each step on the 3D model is shown alongside, and it can be seen that the model has been considerably 'cleaned up' in Step 3.

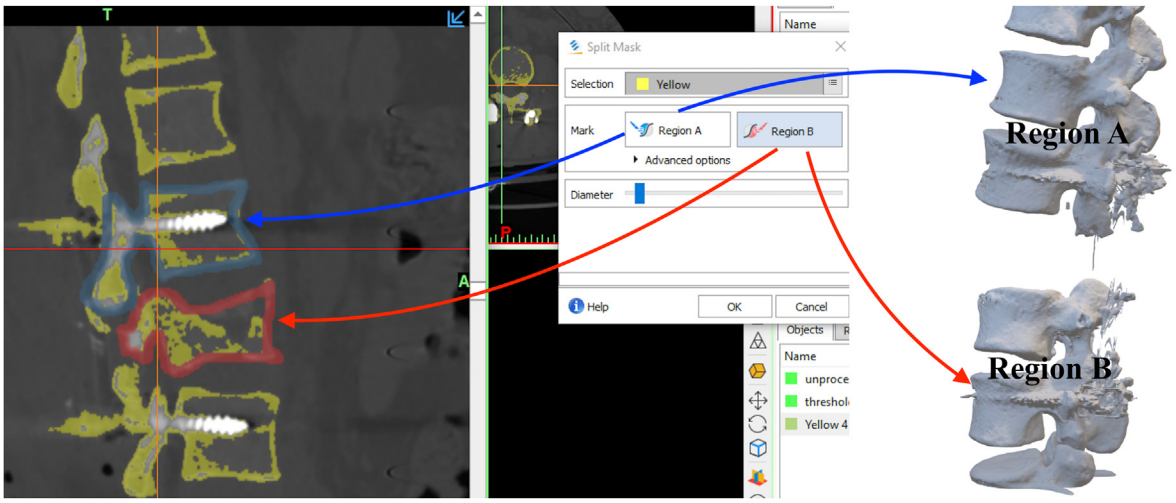

Fig. 4. The 'Split Mask' tool. This tool allows two anatomical regions to be split. The user marks the two regions of interest (A and B) and the software 'splits' the study into two separate segments.

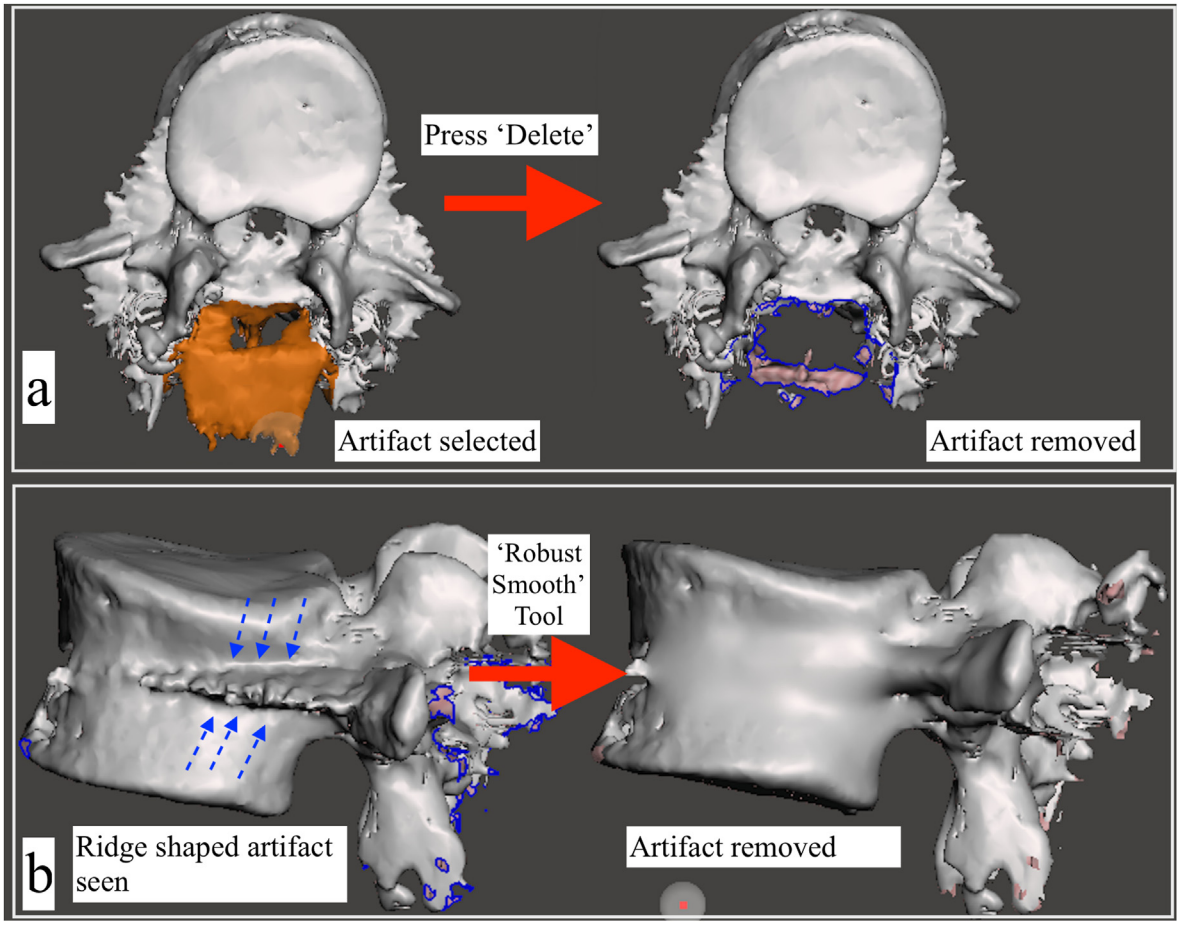

Fig. 5. 3D editing with the Autodesk Meshmixer software a) Metal artifacts surrounding the posterior elements of the vertebra have been select with the 'Select' tool, and are highlighted in orange color. By pressing the 'Delete' button, the selected artifacts have been removed. b) Use of the sculpting tool: a sharp, ridge like metal artifact resulting from the pedicle screw is visualized along the middle and posterior half of the vertebral body (dotted blue arrows). The 'Robust Smooth' tool was used to smoothen out the artifact.

- MinIP reformats are generated by choosing this from the 'Mode' option (this may vary with different software).
- It is seen that although the metal artifacts have decreased, the medial boundaries of the spinal canal are not visualized well,

and whether or not there is a canal breach cannot be identified (Fig. 2a, Step 1).

- Next, the slab thickness is changed from its default value of '2' to '10' (Fig. 2a, Step 2). The boundaries of the spinal canal can now be appreciated well, and it can be appreciated that there is no canal breach (Fig. 2b). What should be the optimal slab thickness for this technique? There is no hard and fast rule, however, it is helpful to increase the slab thickness in 1 mm increments and accept the least slab thickness at which the best visualization is achieved.

c. Advanced image segmentation & editing

As pointed out earlier, the previous two techniques presented in this article simply change how the CT images are viewed on screen, and do not remove or mitigate the artifacts in the dataset. Therefore, if a 3D model (either virtual or 3D printed model) were to be generated from this '*dirty*' dataset (the dataset that contains artifacts), it would contain many artifacts as well. Fortunately, there are many techniques to remove artifacts, and these can be applied before or after a virtual 3D model has been generated. Detailed description of these techniques is beyond the scope of this article, and several free tutorials available online on this subject.

Nonetheless, we would like to present three key concepts, i.e. *3D editing, Segmentation and thresholding*.

3D editing, as the name suggest, refers to techniques can be used to modify images in three dimensions. This term is used loosely to describe a wide variety of techniques. Editing can be performed on the image datasets, as well as virtual 3D models generated from the image datasets.

Segmentation is a process by which an image can be separate in to different segments. For example, an orthopedic surgeon may want to visualize in 3D, the intra-articular extension of a proximal tibial fracture. Using segmentation techniques, the femur and tibia can converted into separate objects, or *segmented,* thereby permitting full visualization of the distal femoral and proximal tibial articular surfaces. *Thresholding* is a segmentation technique by which an image can be filtered according to the intensity of its pixels. In CT images, this is accomplished by filtering images according to their HU values.[29]

Using our previous example of a postoperative lumbar spine CT, we will briefly see how these techniques can be used to address metal artifacts. The MIMICS software (Materialise, Version 21) has been used in this example (a free alternative is the 3D Slicer software, https://www.slicer.org/). Step by step methodology is presented below:

- The CT dataset is imported into the software (MIMICS v. 21). The following steps are followed:
  - o Under the '*Segment*' section, '*Threshold*' is selected. The software detects bone and offers Bone CT threshold (lower limit = 226 HU, upper limit = 3071 HU)settings. If a 3D model were to be generated from the dataset with these threshold settings, many artifacts would be seen (Fig. 3a).
  - o To address this issue, threshold settings are adjusted manually. From our knowledge of the vertebral bone threshold gained in section 4a, the vertebral bone has a minimum HU value of 308 and a maximum HU value of 518. With this information in mind, the threshold setting are adjusted manually to a lower limit of 300 and upper limit of 900 HU. The upper limit is kept on the higher side so that denser vertebral bone from other regions is not left out after thresholding. This is an iterative step, and often one needs to look at the post-

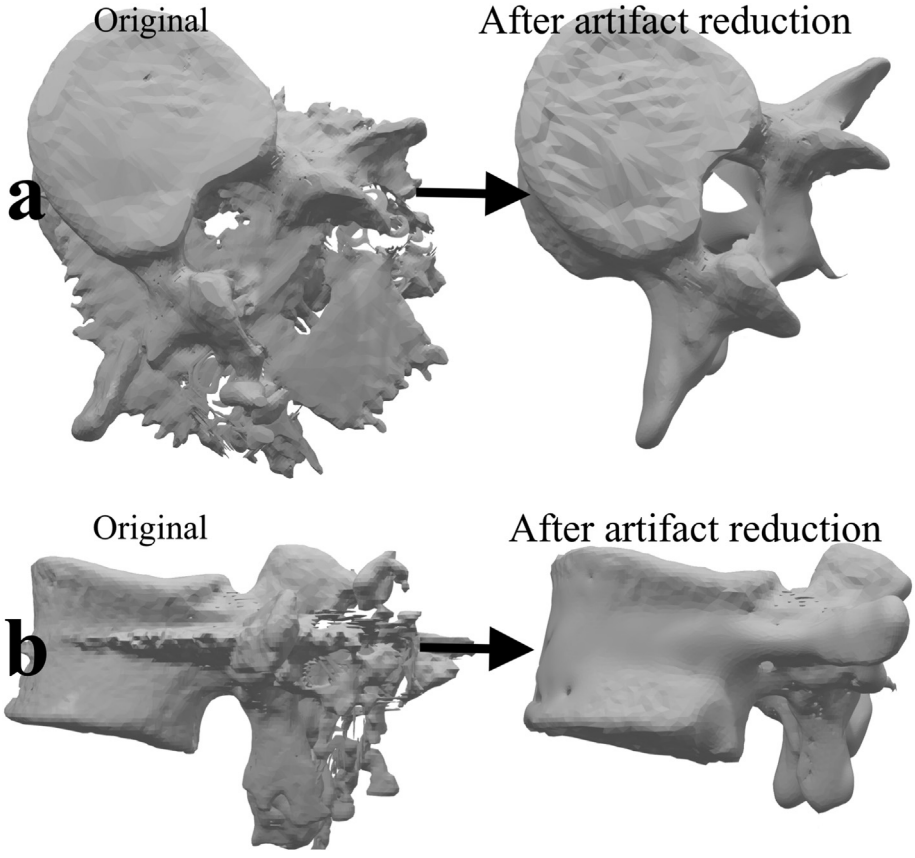

Fig. 6. The 3-D model, before and after removal of the metal artifacts. a) viewed from the top b) viewed from the side.

thresholding output and re-adjust the threshold values until the best images are achieved. A 3D model generated from the manually adjusted threshold shows that many artifacts have been removed. The spinal implants, owing to their higher HU values have also been removed. However, this model still contains numerous artifacts as needs to be 'cleaned up' more (Fig. 3b).

- The next step is to perform another segmentation technique termed as '*Region Growing*'. The user selects an initial point, known as the 'seed point'. The software will then iteratively select all the pixels within a pre-defined range. To perform this step, the user clicks on a point within the vertebral bone. The software will then perform segmentation. A 3D model generated from this step has much lesser artifacts as compared to the previous two steps (Fig. 3c).
- What if the orthopedic surgeon only wanted to print the normal vertebra proximal to the fractured vertebra? This can be accomplished by a tool known as the 'Split Mask'. The user draws outlines of the vertebral proximal to the fracture, and the fractured vertebra itself. The software then 'splits' the image into two *split* parts. One split part contains the fractured vertebra and other vertebrae distal to it, whereas the other split part contains vertebrae proximal to the fractured vertebra. By repeating this step, one can isolate the vertebra of interest (Fig. 4).
- The vertebra of interest has now been isolated, but it contains artifacts from the metal implants.

- The model is now imported into the Autodek Meshmixer software (https://www.meshmixer.com/)for cleaning up the artifacts. Detailed tutorials on this software are available on the internet. A brief overview is presented here:
  - Unwanted islands can be removed from the model by selecting them and pressing '*delete*' (Fig. 5a).
  - Holes in the model can be addressed by selecting the area around the holes, and then selecting the '*erase and fill*' option.
  - A variety of sculpting tools are also available to '*sculpt*' the model to its desired shape. Brushes such as the 'Flatten' and 'RobustSmooth', can be used to remove surface irregularities (Fig. 5b). These processes are iterative, and time consuming, and the user's experience with the software is reflected in the 'cleaned-up' final model (Fig. 6).

It must be remembered that 3D models edited using these tools would not reflect the anatomy accurately, and therefore, should not be used for precision measurements. However, they can be used for three dimensional visualization, and also for 3-D printing.

5. Conclusion

Metal artifacts can hamper visualization of CT images. When ordering a CT scan for patients with metal hardware *in-situ*, the orthopedic surgeon must clearly spell out the need for metal artifact reduction, which can be accomplished by the radiographer by a variety of commercially available solutions. In the event that metal artifact reduction has not been addressed, the three techniques presented in this article may be of use in visualization or preparing the image data for 3-D printing.

Abbreviations

CT	Computed Tomography
DICOM	Digital Imaging and Communication in Medicine
MARS	Metal Artifact Reduction Sequence
MinIP	Minimum Intensity Projection
MIP	Maximum Intensity Projection
MPR	Multiplanar Reformation
MRI	Magnetic Resonance Imaging
VR	Volume Rendering
SNR	Signal to Noise Ratio

References

1. Crijns TJ, Mellema JJ, Özkan S, Ring D, Chen NC, Science of Variation Group. Classification of tibial plateau fractures using 3DCT with and without subtraction of unfractured bones. *Injury*. 2020;51(11):2686–2691. https://doi.org/10.1016/j.injury.2020.07.038.
2. Tarallo L, Micheloni GM, Mazzi M, Rebeccato A, Novi M, Catani F. Advantages of preoperative planning using computed tomography scan for treatment of malleolar ankle fractures. *World J Orthoped*. 2021;12(3):129–139. https://doi.org/10.5312/wjo.v12.i3.129.
3. Haleem A, Javaid M. Role of CT and MRI in the design and development of orthopaedic model using additive manufacturing. *J Clin Orthop Trauma*. 2018;9(3):213–217. https://doi.org/10.1016/j.jcot.2018.07.002.
4. Elnahal WA, Vetharajan N, Mohamed B, Acharya M, Chesser TJS, Ward AJ. Routine postoperative computed tomography scans after pelvic fracture fixation: a necessity or a luxury? *J Orthop Trauma*. 2018;32(Suppl 1):S66–S71. https://doi.org/10.1097/BOT.0000000000001092.
5. Mustonen AOT, Koivikko MP, Kiuru MJ, Salo J, Koskinen SK. Postoperative MDCT of tibial plateau fractures. *AJR Am J Roentgenol*. 2009;193(5):1354–1360. https://doi.org/10.2214/AJR.08.2260.
6. Ghodasara N, Yi PH, Clark K, Fishman EK, Farshad M, Fritz J. Postoperative spinal CT: what the radiologist needs to know. *Radiographics*. 2019;39(6):1840–1861. https://doi.org/10.1148/rg.2019190050.
7. Roth TD, Maertz NA, Parr JA, Buckwalter KA, Choplin RH. CT of the hip prosthesis: appearance of components, fixation, and complications. *Radiographics*. 2012;32(4):1089–1107. https://doi.org/10.1148/rg.324115183.
8. Mushtaq N, To K, Gooding C, Khan W. Radiological imaging evaluation of the failing total hip replacement. *Front Surg*. 2019;6. https://doi.org/10.3389/fsurg.2019.00035.
9. Kleinlugtenbelt YV, Scholtes VAB, Toor J, et al. Does computed tomography change our observation and management of fracture non-unions? *Arch Bone Jt Surg*. 2016;4(4):337–342.
10. Fisher JS, Kazam JJ, Fufa D, Bartolotta RJ. Radiologic evaluation of fracture healing. *Skeletal Radiol*. 2019;48(3):349–361. https://doi.org/10.1007/s00256-018-3051-0.
11. Coughlin MJ, Kaz A. Correlation of harris mats, physical exam, pictures, and radiographic measurements in adult flatfoot deformity. *Foot Ankle Int*. 2009;30(7):604–612. https://doi.org/10.3113/FAI.2009.0604.
12. Barmeir E, Dubowitz B, Roffman M. Computed tomography in the assessment and planning of complicated total hip replacement. *Acta Orthop Scand*. 1982;53(4):597–604. https://doi.org/10.3109/17453678208992265.
13. Kalender WA, Hebel R, Ebersberger J. Reduction of CT artifacts caused by metallic implants. *Radiology*. 1987;164(2):576–577. https://doi.org/10.1148/radiology.164.2.3602406.
14. Lee M-J, Kim S, Lee S-A, et al. Overcoming artifacts from metallic orthopedic implants at high-field-strength MR imaging and multi-detector CT. *Radiographics*. 2007;27(3):791–803. https://doi.org/10.1148/rg.273065087.
15. Barrett JF, Keat N. Artifacts in CT: recognition and avoidance. *Radiographics*. 2004;24(6):1679–1691. https://doi.org/10.1148/rg.246045065.
16. Boas FE, Fleischmann D. Evaluation of two iterative techniques for reducing metal artifacts in computed tomography. *Radiology*. 2011;259(3):894–902. https://doi.org/10.1148/radiol.11101782.
17. Engel KJ, Herrmann C, Zeitler G. X-ray scattering in single- and dual-source CT. *Med Phys*. 2008;35(1):318–332. https://doi.org/10.1118/1.2820901.
18. Matsumoto K, Jinzaki M, Tanami Y, Ueno A, Yamada M, Kuribayashi S. Virtual monochromatic spectral imaging with fast kilovoltage switching: improved image quality as compared with that obtained with conventional 120-kVp CT. *Radiology*. 2011;259(1):257–262. https://doi.org/10.1148/radiol.11100978.
19. Haramati N, Staron RB, Mazel-Sperling K, et al. CT scans through metal scanning technique versus hardware composition. *Comput Med Imag Graph*. 1994;18(6):429–434. https://doi.org/10.1016/0895-6111(94)90080-9.
20. Graser A, Johnson TRC, Chandarana H, Macari M. Dual energy CT: preliminary observations and potential clinical applications in the abdomen. *Eur Radiol*. 2009;19(1):13–23. https://doi.org/10.1007/s00330-008-1122-7.
21. Karçaaltıncaba M, Aktaş A. Dual-energy CT revisited with multidetector CT: review of principles and clinical applications. *Diagn Interv Radiol*. 2011;17(3):181–194. https://doi.org/10.4261/1305-3825.DIR.3860-10.0.
22. McCollough CH, Leng S, Yu L, Fletcher JG. Dual- and multi-energy CT: principles, technical approaches, and clinical applications. *Radiology*. 2015;276(3):637–653. https://doi.org/10.1148/radiol.2015142631.
23. Axente M, Paidi A, Von Eyben R, et al. Clinical evaluation of the iterative metal artifact reduction algorithm for CT simulation in radiotherapy. *Med Phys*. 2015;42(3):1170–1183. https://doi.org/10.1118/1.4906245.
24. Wagenaar D, van der Graaf ER, van der Schaaf A, Greuter MJW. Quantitative comparison of commercial and non-commercial metal artifact reduction techniques in computed tomography. *PloS One*. 2015;10(6), e0127932. https://doi.org/10.1371/journal.pone.0127932.
25. Masoudi S, Harmon SA, Mehralivand S, et al. Quick guide on radiology image

pre-processing for deep learning applications in prostate cancer research. *J Med Imaging*. 2021;8(1), 010901. https://doi.org/10.1117/1.JMI.8.1.010901.
26. Goldman LW. Principles of CT and CT technology. *J Nucl Med Technol*. 2007;35(3):115–128. https://doi.org/10.2967/jnmt.107.042978. quiz 129-130.
27. Whalen B. The slice is right (an exercise in CT windowing). *Can J Med Radiat Technol*. 2003;34(4):5–10. https://doi.org/10.1016/S0820-5930(09)60033-5.
28. Cody DD. AAPM/RSNA physics tutorial for residents: topics in CT. Image processing in CT. *Radiographics*. 2002;22(5):1255–1268. https://doi.org/10.1148/radiographics.22.5.g02se041255.
29. Deserno TM. Fundamentals of medical image processing. In: Kramme R, Hoffmann K-P, Pozos RS, eds. *Springer Handbook of Medical Technology*. Springer Handbooks. Springer; 2011:1139–1165. https://doi.org/10.1007/978-3-540-74658-4_62.